« *Advances on Giant Nuclear Monopole Excitations and Application to Multimessenger Astrophysics* »,
11-15 juillet 2022, ECT Trento*

Nuclear incompressibility and sound speed in uniform matter and finite nuclei, impact for neutron stars.

Jérôme MARGUERON
IP2I Lyon

Take-home message: The reproduction of E_{GMR} in Pb and Sn may require specific values for $Q_{sat.}$ The suggested values are quite different from existing models.

In collaboration with:

Guilherme Grams (IAA Bruxelles)
Rahul Somasundaram (IP2I Lyon)
Elias Khan (IJCLab Orsay)

Recent results in:

Grams, Somasundaram, JM, Khan,
arXiv 2207.01884 (nucl-th)

Anatomy of a neutron star (NS)

NS are largely investigated thanks to our knowledge in nuclear and hadron physics.

Atmosphere: H, He

Outer crust: nuclear clusters+electons

Radius $\approx 11 - 14$km

Mass $\approx 1.2 - 2.2 M_\odot$

Inner crust: nuclear clusters+electrons+neutron gas

Outer core: uniform nuclear matter (n, p, e, μ)

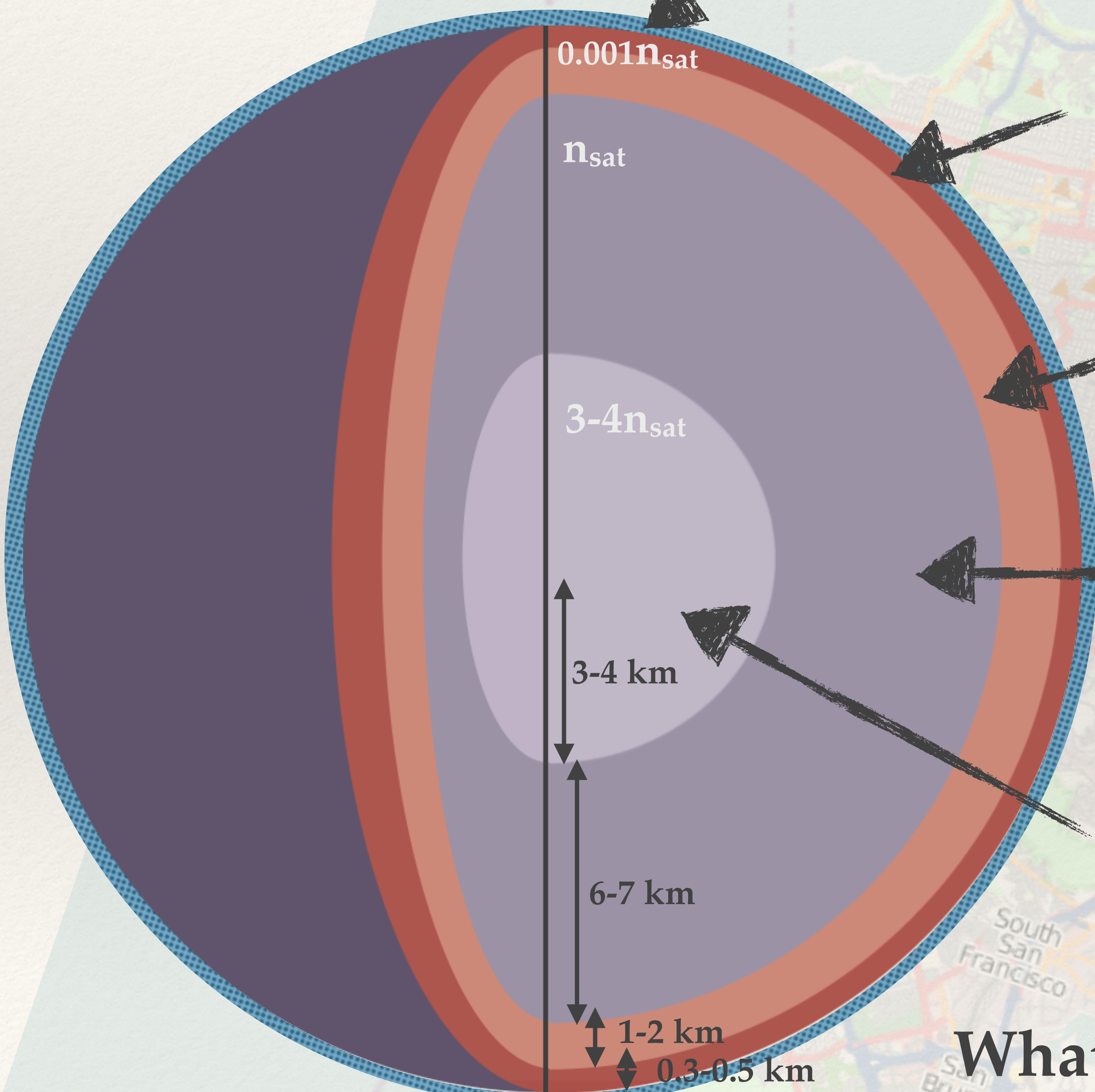

Inner core: unknown composition

NS **radius** provides information about the **core** mostly, but there is also a contribution from the crust (10%).

What is hiding in the inner core of NS?

EoS [nuclear] <=> NS (M,R) [astro]

Properties of extreme matter

P(n)

Tolmann-Oppenheimer-Volkov (TOV) GR equations

(M,R)(n_c)

Astrophysical observations

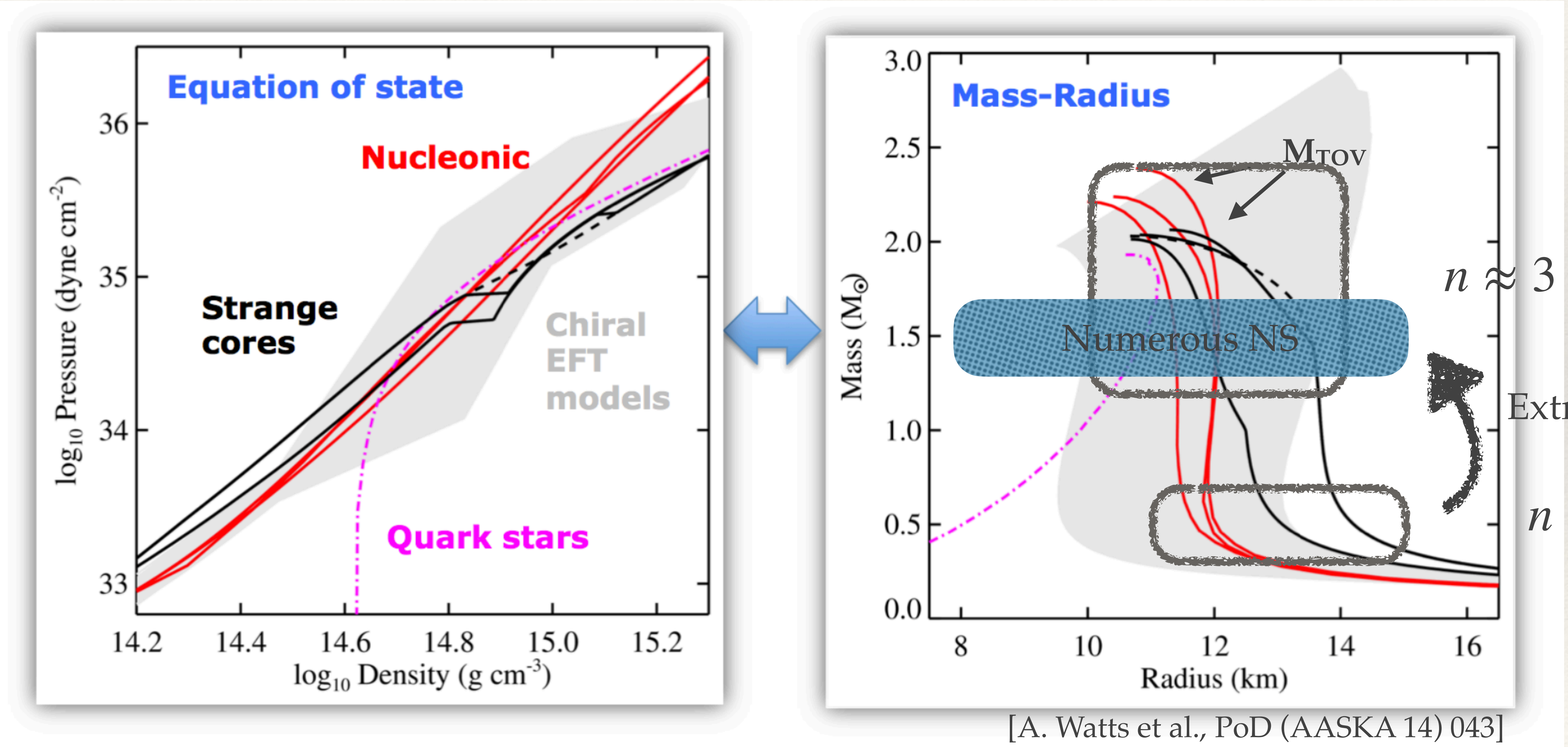

$n \approx 3 - 6n_{sat}$

Extrapolation

$n \approx n_{sat}$

[A. Watts et al., PoD (AASKA 14) 043]

Reverse engineering, Bayesian statistics

Inferring the EoS from the low-density nuclear regime

Opposite to determining the dense matter EoS from high density (perturbative QCD).

See Annala, Kurkela in PRL 117, 042501 (2016), PRL 120, 172703 (2018), Nat. Phys. 16, 907 (2020)

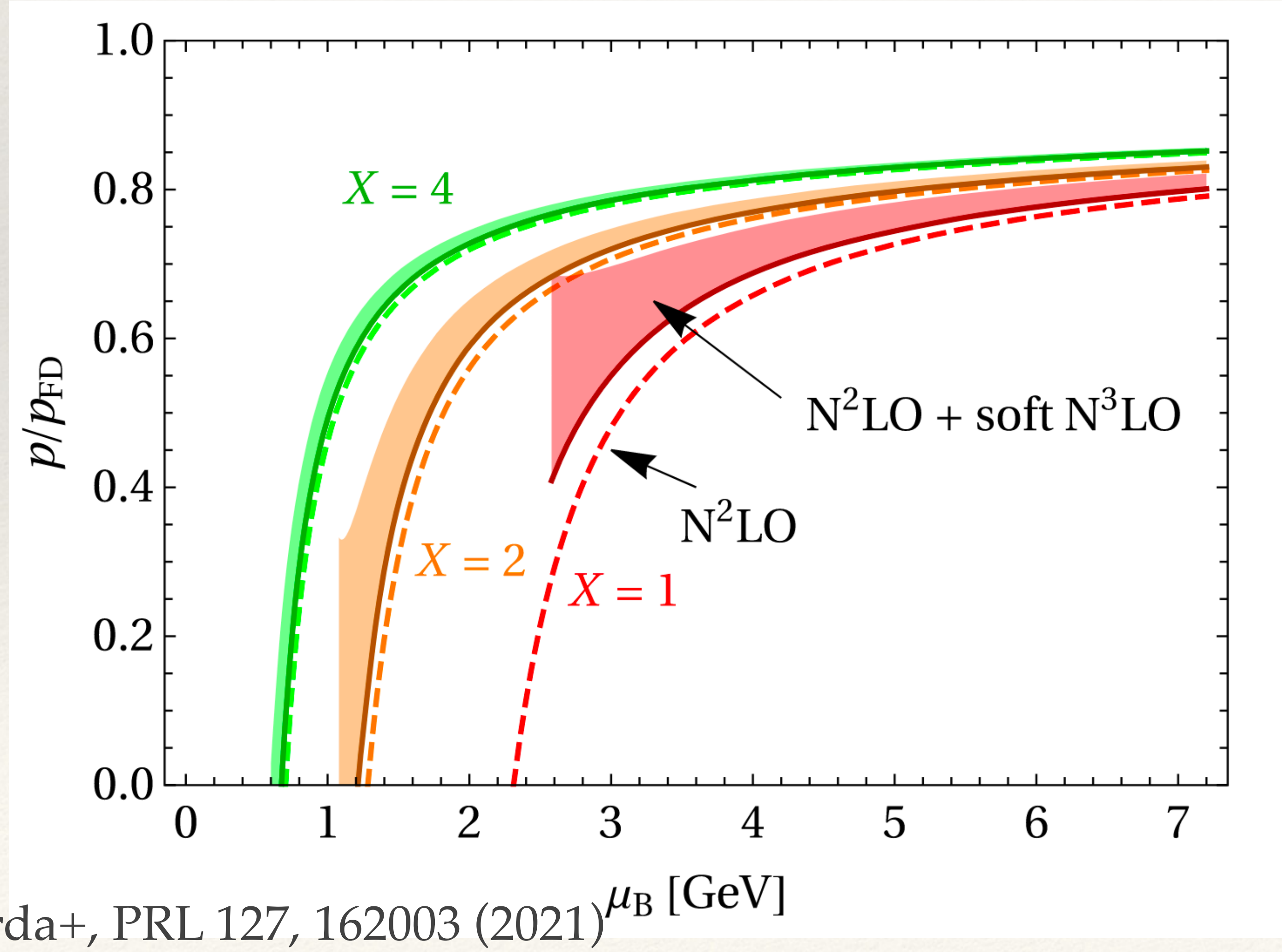

Gorda+, PRL 127, 162003 (2021)

Extrapolation to low density:

Komoltsev & Kurkela, PRL 128, 202701 (2022)

Application to neutron star:

Gorda+, arXiv:2204.11877
Somasundaram+, arXiv:2204.14039

Meta-model for the nuclear EoS

[Baillot d'Étivaux+, ApJ 2019]

The **nuclear empirical parameters** (NEP) capture the properties of the EoS around n_{sat}:

Less known NEP — Unknown NEP

$$e_{sat} = E_{sat} + \frac{1}{2}K_{sat}x^2 + \frac{1}{6}Q_{sat}x^3 + \frac{1}{24}Z_{sat}x^4 + \dots$$

$$e_{sym} = E_{sym} + L_{sym}x + \frac{1}{2}K_{sym}x^2 + \frac{1}{6}Q_{sym}x^3 + \frac{1}{24}Z_{sym}x^4 + \dots$$

with $\delta = (n_n - n_p)/(n_n + n_p)$ and $x = (n - n_{sat})/(3n_{sat})$

JM, Casali, Gulminelli, PRC 97, 025805 (2018)

Semi-agnostic approach (Meta-model):

$$e(n,\delta) = t(n,\delta) + v(n,\delta)$$

Kinetic energy (Fermi gas)

Potential energy

$$v(n,\delta) = \sum_{\alpha=0}^{N} \left(v_\alpha^{is} + \delta^2 v_\alpha^{iv}\right) \frac{x^\alpha}{\alpha!} u(x),$$

Directly related to NEP

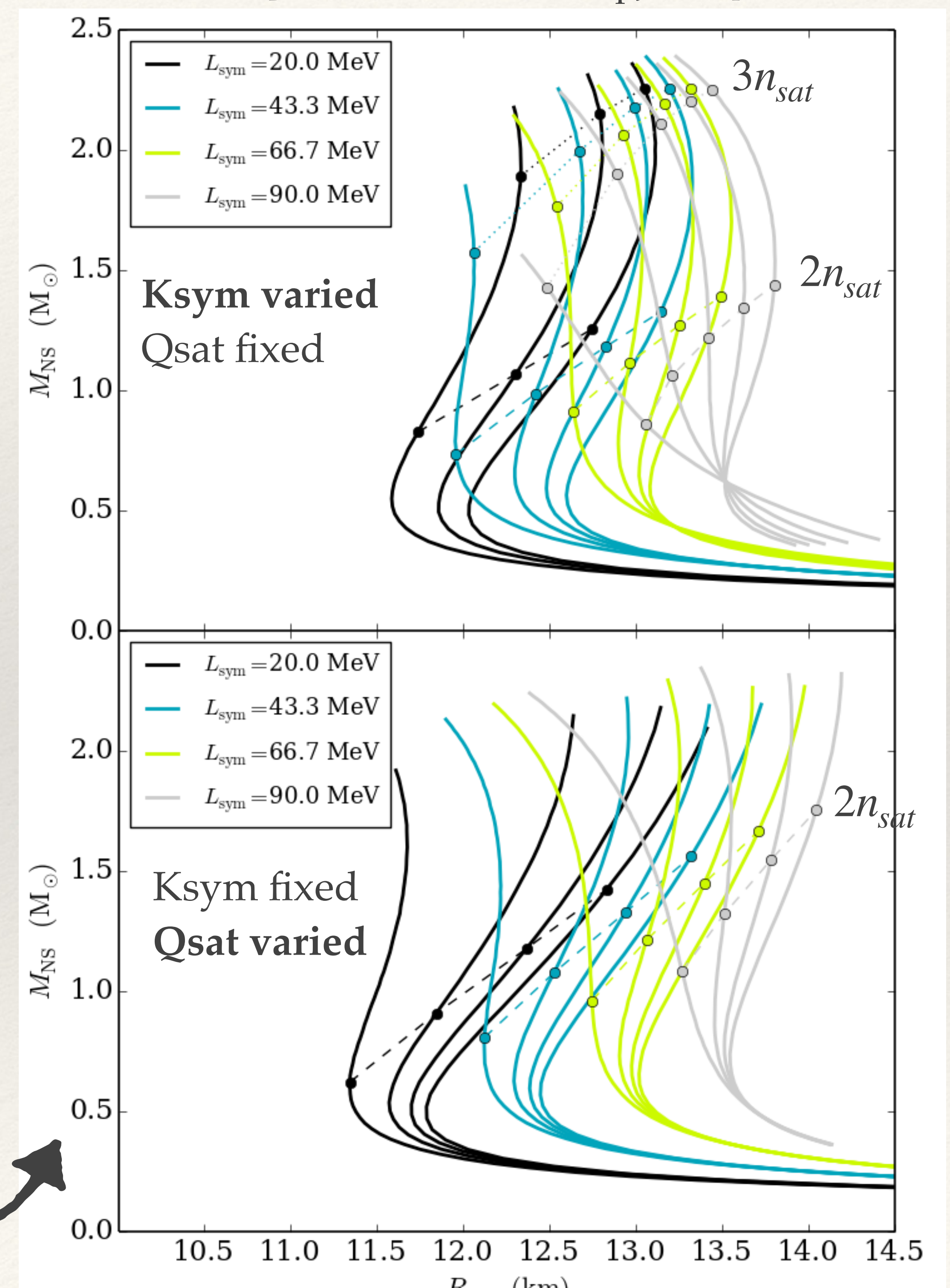

Impact of K_{sat} & Q_{sat} on MR relation

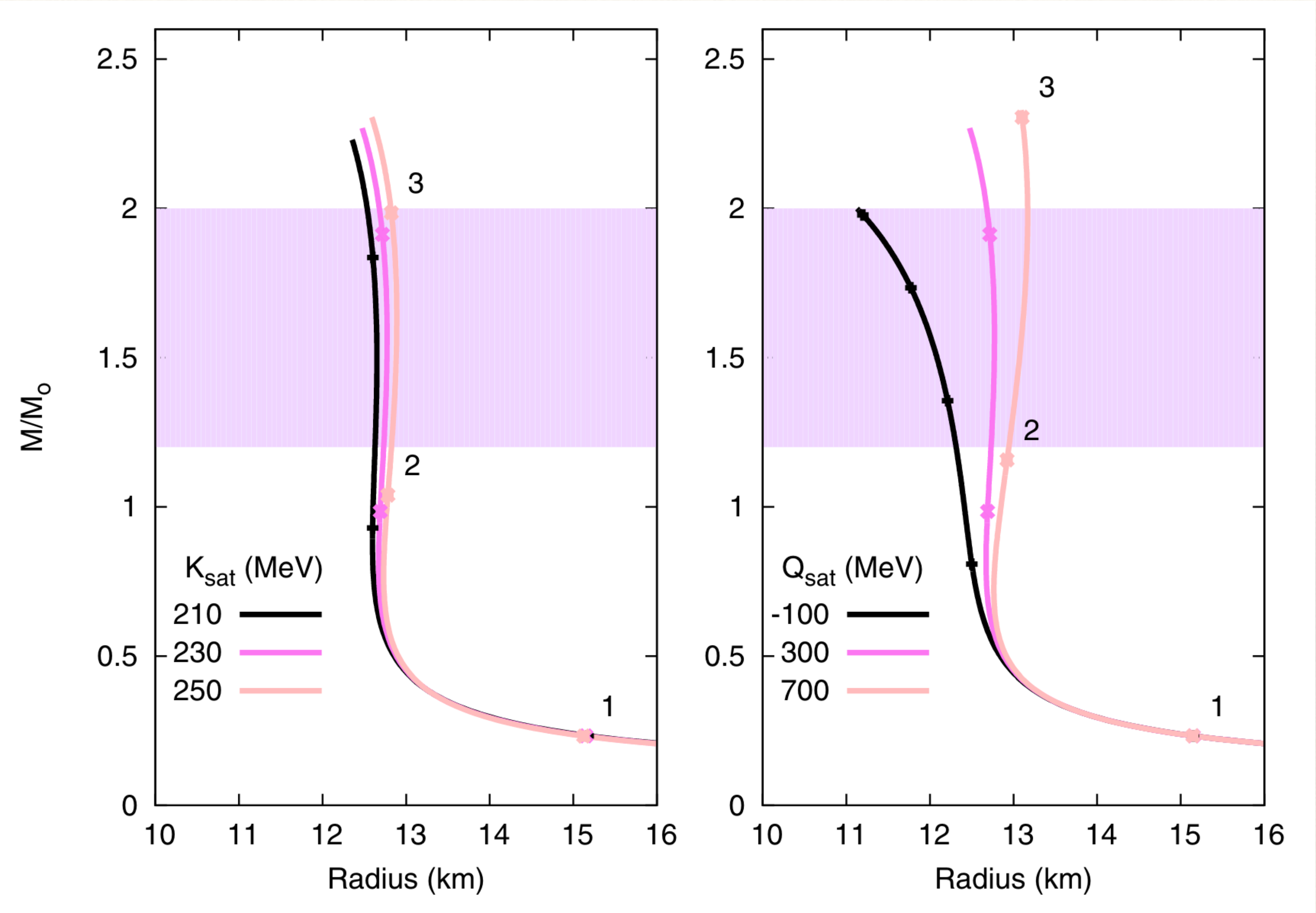

JM, Casali, Gulminelli, PRC 97, 025806 (2018)

Impact of isovector NEP on MR relation

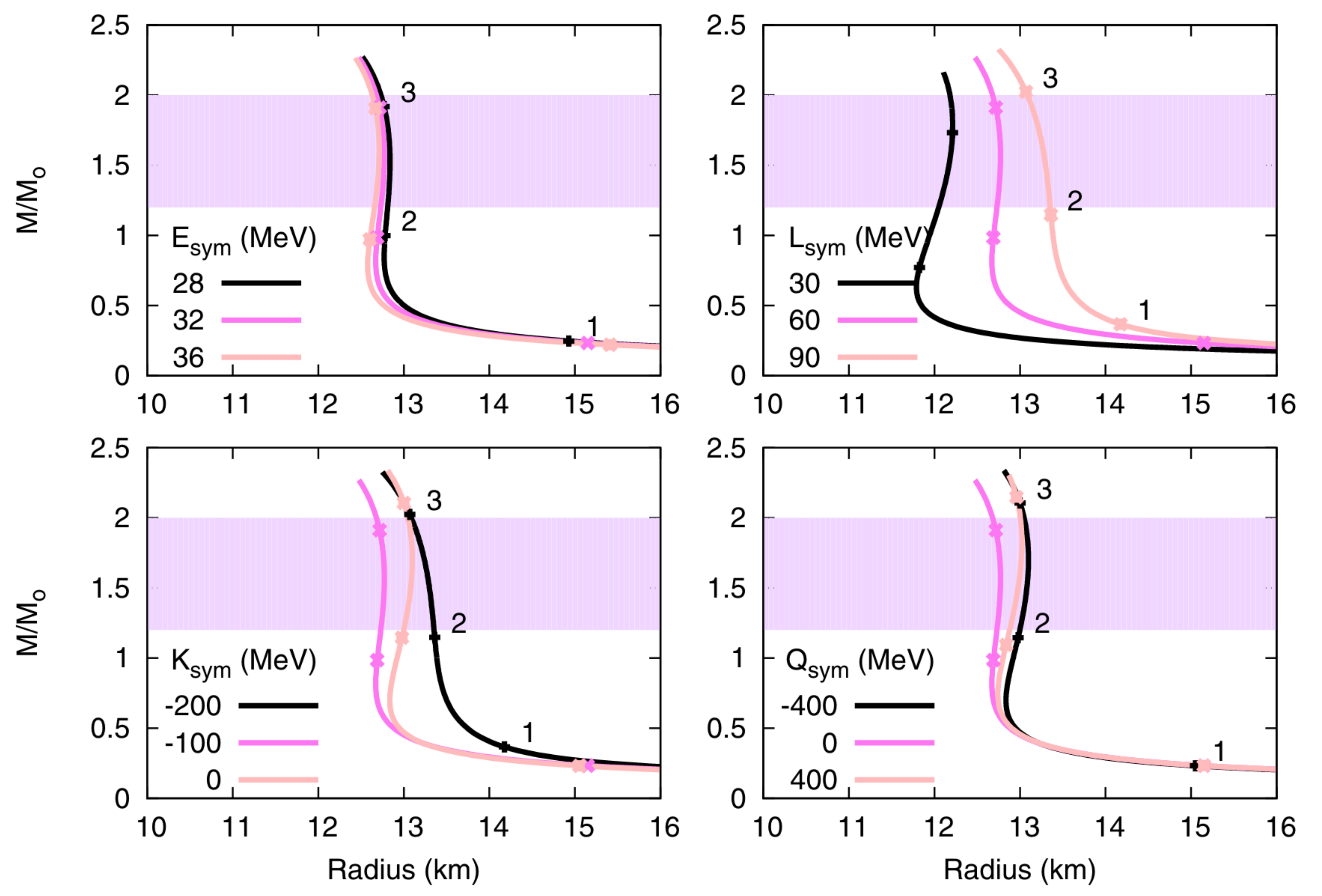

JM, Casali, Gulminelli, PRC 97, 025806 (2018)

Inferring nuclear properties from E_{ISGMR}

Correlation between: Nuclei properties ⟷ Uniform matter properties

Blaizot, PR 64, 171 (1980)

$$E_{GMR} = \sqrt{\frac{m_1}{m_{-1}}}$$

$$K(n) = 9n\frac{\partial^2 \epsilon(n)}{\partial n^2}$$

$$K_{\text{sat}} = K(n = n_{\text{sat}})$$

m_1 and m_{-1} are computed from Constrained HF

$$M_c = 3n_c K'(n = n_c)$$

Khan, JM, Vidaña, PRL 109, 092501 (2012)
Khan, JM, PRC 88, 034319 (2013)

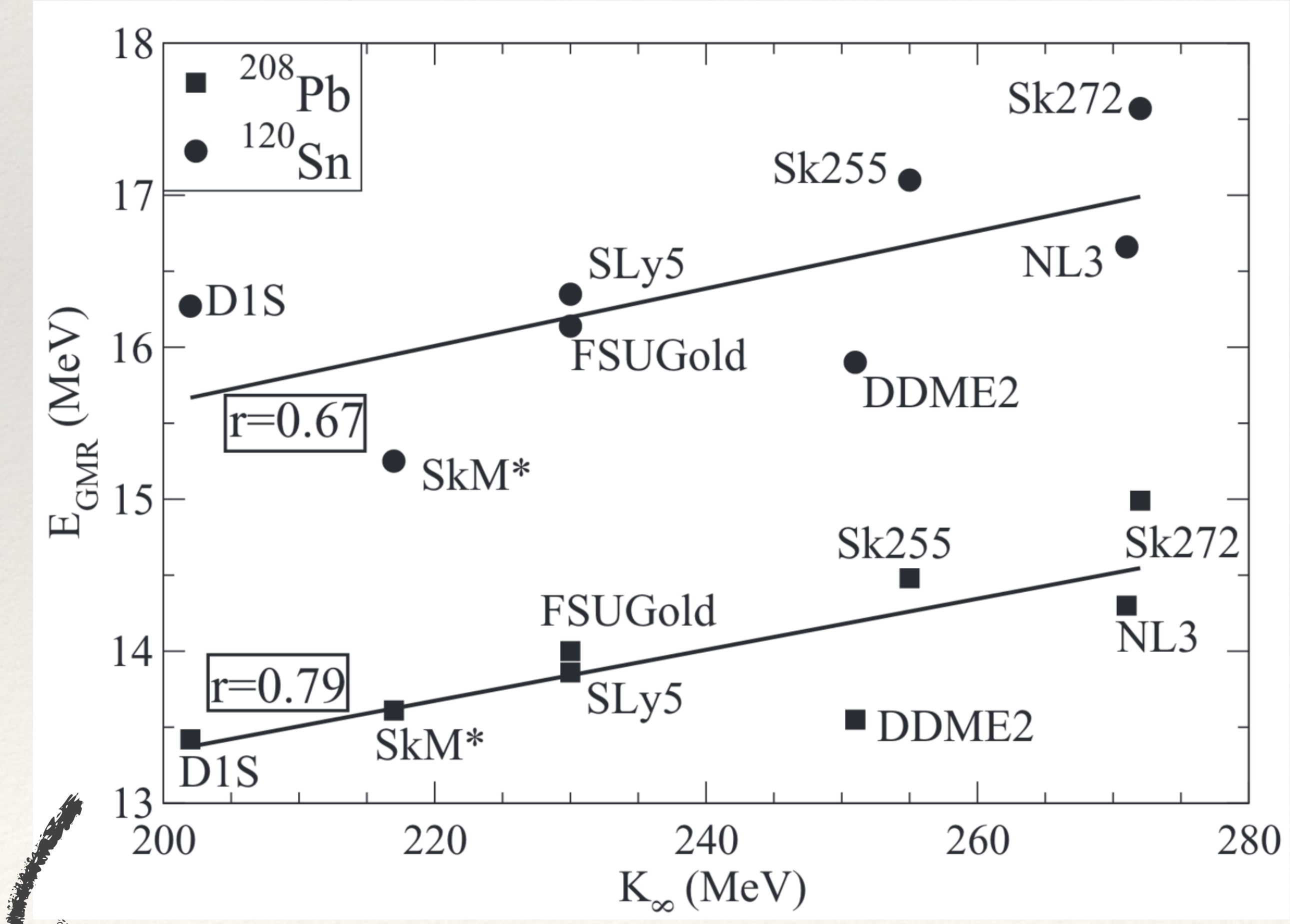

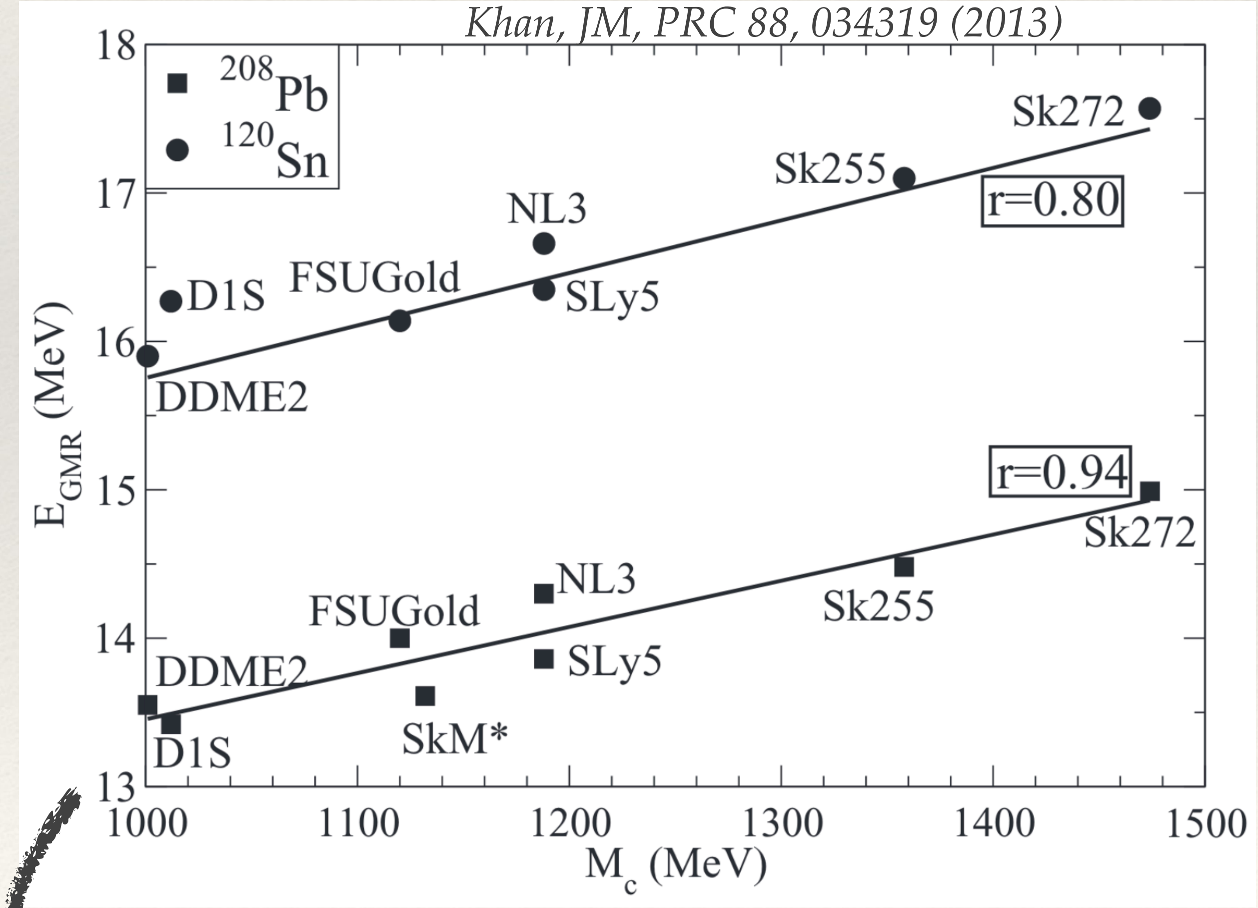

$$K_{sat} = 230 \pm 30 \text{ MeV}$$

$$M_c = 1050 \pm 100 \text{ MeV}$$

From n_c to n_{sat}

Running of several models (Skyrme, Gogny, RMFs):

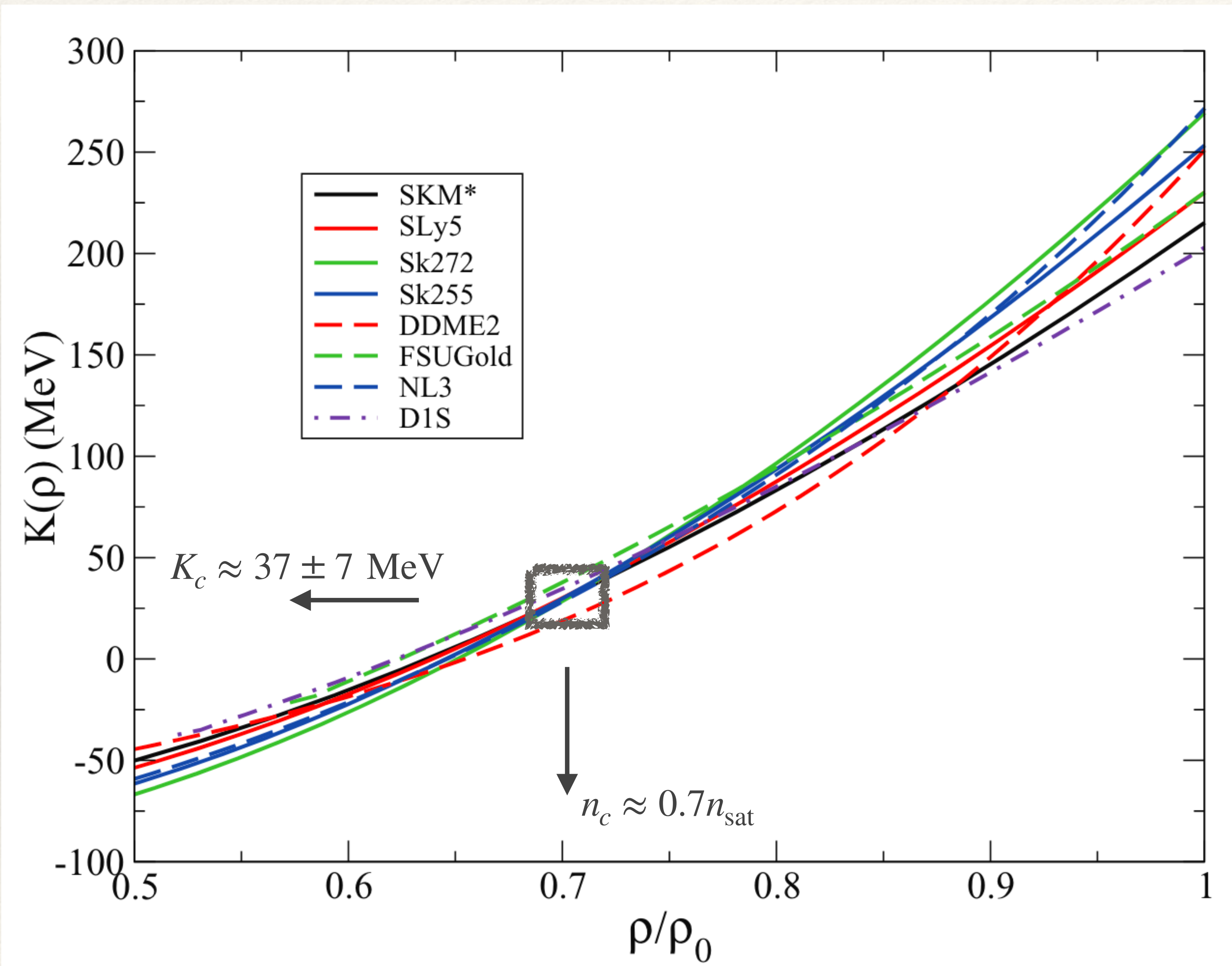

We have:

$$K(n) = K_c + K'(n - n_c)$$

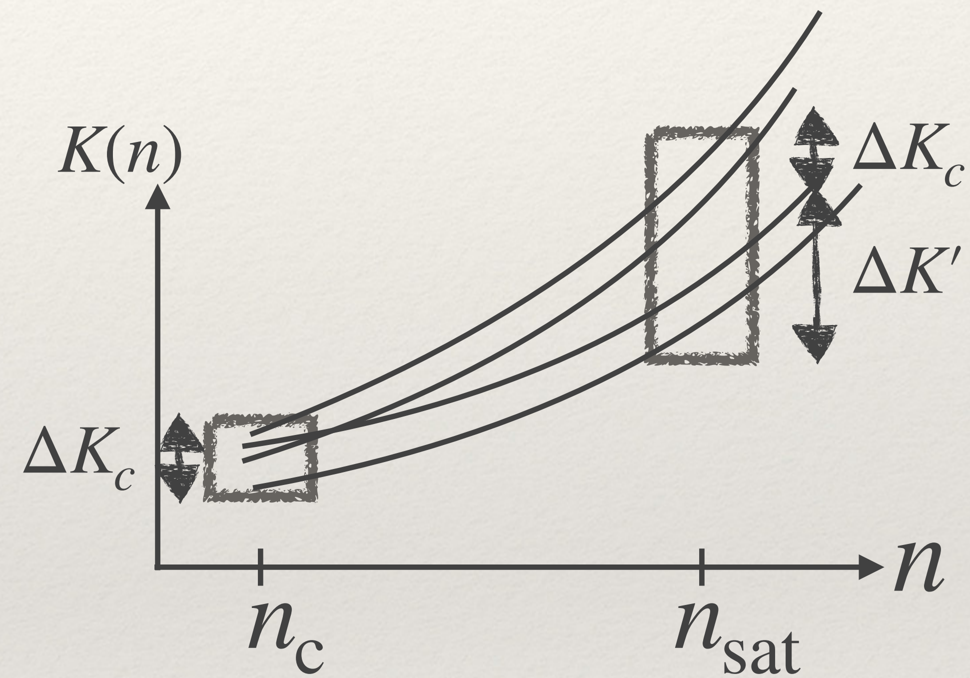

$$\Delta K' \propto Q_{sat}$$

-> The uncertainty in K_{sat} is induced by Q_{sat}.

General result: the uncertainty in a NEP is often generated by higher order NEPs.

JM & Gulminelli, PRC 99, 025806 (2019)

Q_{sat} is model dependent

JM, Casali, Gulminelli, PRC 97, 025805 (2018)

Model (N_α)	Der. order	E_{sat} (MeV) 0	E_{sym} (MeV) 0	n_{sat} (fm^{-3}) 1	L_{sym} (MeV) 1	K_{sat} (MeV) 2	K_{sym} (MeV) 2	Q_{sat} (MeV) 3	Q_{sym} (MeV) 3	Z_{sat} (MeV) 4	Z_{sym} (MeV) 4	m^*_{sat}/m	$\Delta m^*_{sat}/m$	κ_v	K_τ (MeV)
							Phenomenological approaches								
Skyrme	Average	−15.88	30.25	0.1595	47.8	234	−130	−357	378	1500	−2219	0.73	0.08	0.46	−344
(16)	σ	0.15	1.70	0.0011	16.8	10	66	22	110	169	617	0.10	0.24	0.27	25
Skyrme	Average	−15.87	30.82	0.1596	49.6	237	−132	−349	370	1448	−2175	0.77	0.127	0.44	−354
(35)	σ	0.18	1.54	0.0039	21.6	27	89	89	188	510	1069	0.14	0.310	0.37	45
RMF	Average	−16.24	35.11	0.1494	90.2	268	−5	−2	271	5058	−3672	0.67	−0.09	0.40	−549
(11)	σ	0.06	2.63	0.0025	29.6	34	88	393	357	2294	1582	0.02	0.03	0.06	153
RHF	Average	−15.97	33.97	0.1540	90.0	248	128	389	523	5269	−9956	0.74	−0.03	0.34	−572
(4)	σ	0.08	1.37	0.0035	11.1	12	51	350	237	838	4156	0.03	0.01	0.07	169
Total	Average	−16.03	33.30	0.1543	76.6	251	−3	13	388	3925	−5268	0.72	0.01	0.39	−492
(50)	σ_{tot}	0.20	2.65	0.0054	29.2	29	132	431	289	2270	4282	0.09	0.20	0.22	166
	Min	−16.35	26.83	0.1450	9.9	201	−394	−748	−86	−903	−16 916	0.38	−0.47	0.00	−835
	Max	−15.31	38.71	0.1746	122.7	355	213	950	846	9997	−5	1.11	1.02	2.02	−254
							Ab initio approaches								
APR	Average	−16.0	33.12	0.16	50.0	270	−199	−665	923	337	−2053	1.0	0.0	0.0	−376
(1)	σ	[a]	0.30	[a]	1.3	2	13	30	67	94	125	[a]	[a]	[a]	30
Chiral EFT	Average	−15.16	32.01	0.171	48.1	214	−172	−139	−164	1306	−2317				−428
Drischler 2016	σ_{tot}	1.24	2.09	0.016	3.6	22	40	104	234	214	379				63
(7)	Min	−16.92	28.53	0.140	43.9	182	−224	−310	−640	901	−2961				−534
	Max	−13.23	34.57	0.190	53.5	242	−108	24	96	1537	−1750				−334

Skyrme / RMF / RHF / APR / xEFT

[a]This parameter is fixed.

Correlation between K_{sat} and Q_{sat}

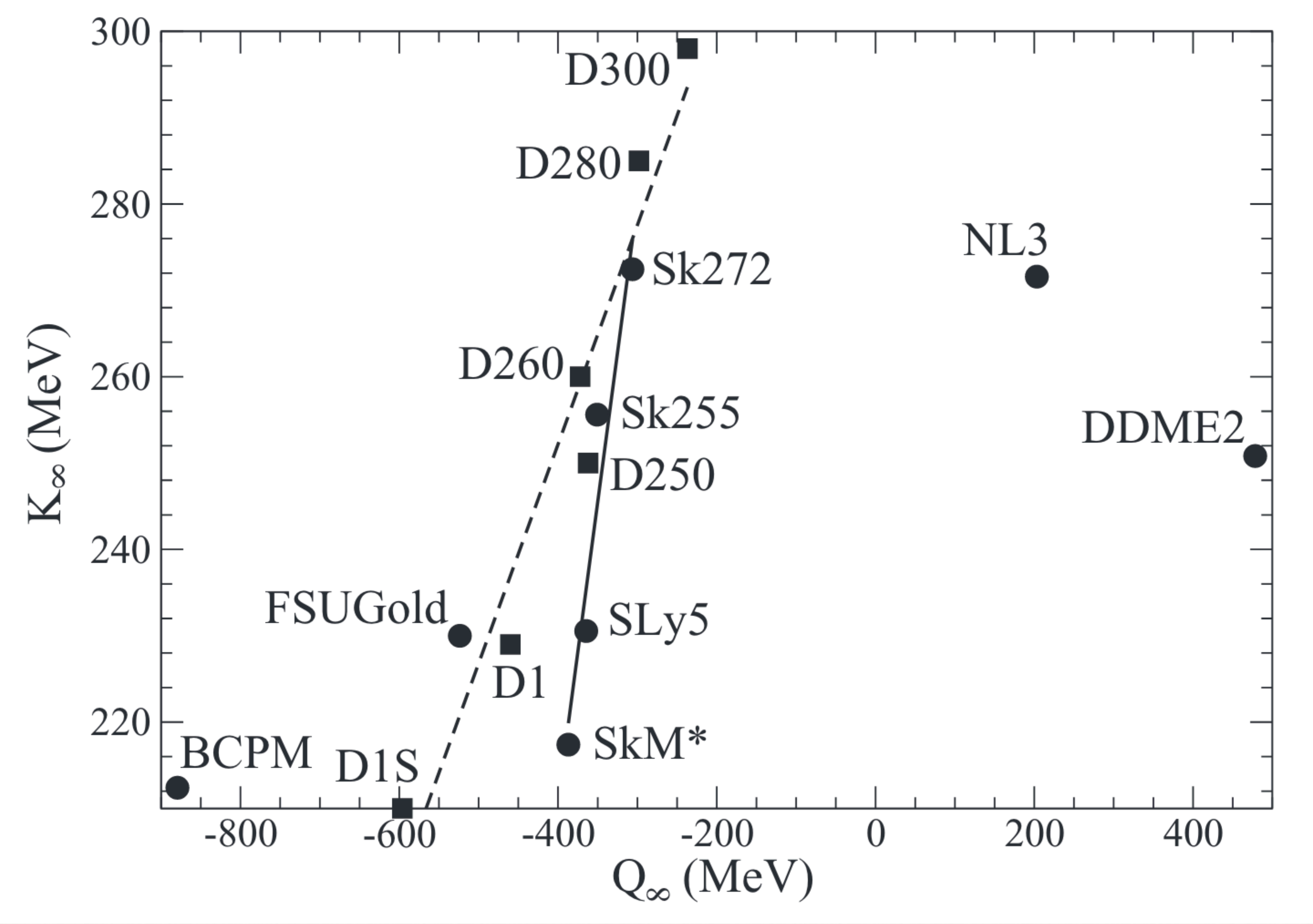

Khan, JM, Vidaña, PRL 109, 092501 (2012)
Khan, JM, PRC 88, 034319 (2013)

Correlation between K_{sat} and Q_{sat}

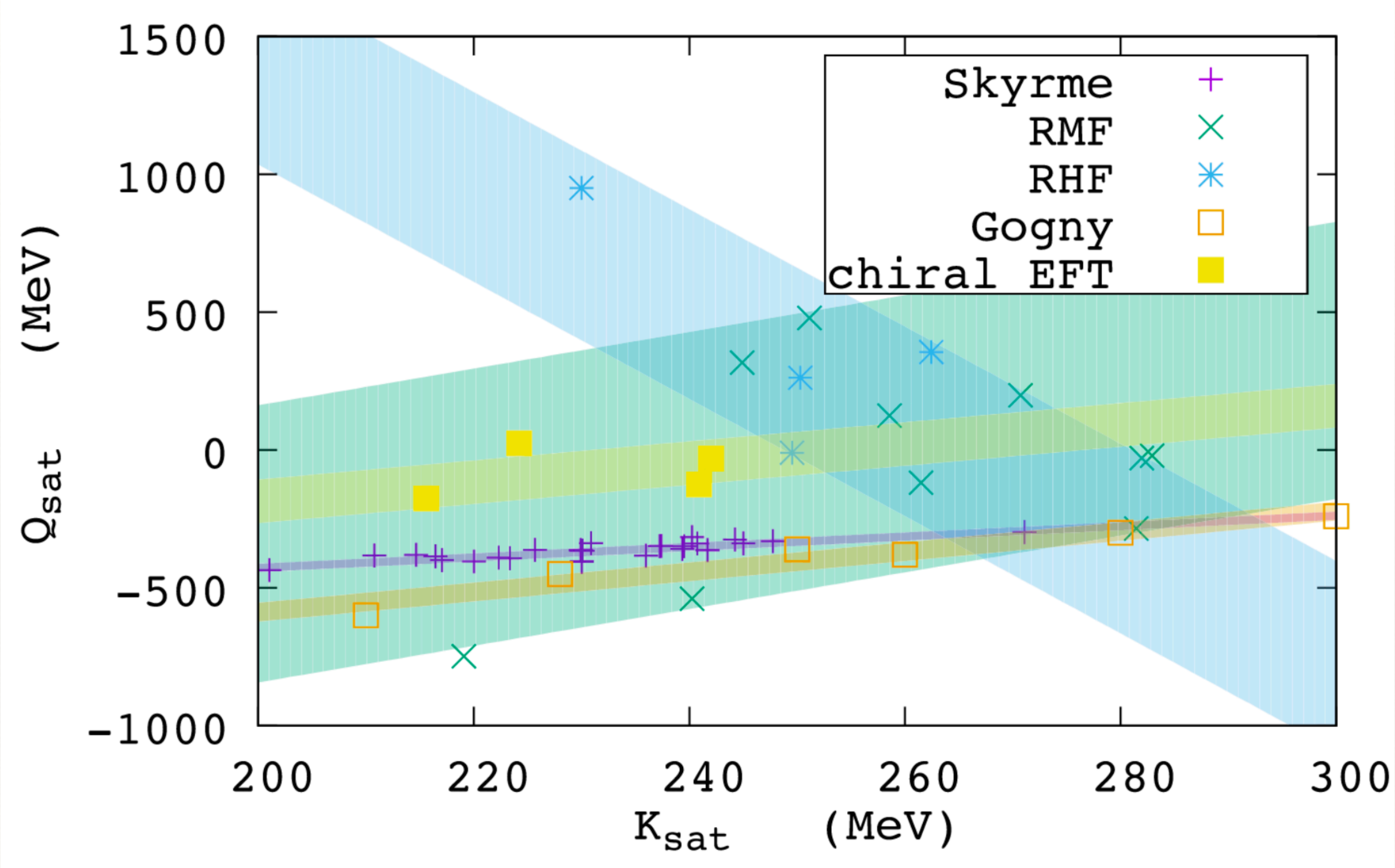

JM, Casali, Gulminelli, PRC 97, 025805 (2018)

Improved nuclear modeling

Issues: Model dependence of K_{sat}.
Better description of E_{GMR}/K_A over the nuclear chart:
soft Sn / hard Pb puzzle.

Piekarewicz & Centelles, PRC 79, 054311 (2009)
Elias Khan, PRC 80, 011307 and 057302 (2009)
See talk of A. Pastore

May be due to the theoretical tool -> weak impact for dense matter EoS.

May be due to the interaction -> possible large impact for dense matter EoS.
More precisely may be due to Q_{sat}.

-> if Q_{sat} is known: better extrapolation of the EoS for NS matter

Requirement: The correlation between K_{sat} and Q_{sat} shall be broken.

How? -> increase the number of parameters in the phenomenological nuclear force.
-> adopt a meta-model approach.

Leptodermous expansion for e_A

Liquid-drop model:

$$e_A(n_A, \delta_A) = e_{UM}(n_A, \delta_A) + E_{Coul}\frac{Z^2}{A^{4/3}} + E_{surf}(\delta_A)A^{-1/3} + \ldots$$

where $n_A = 3A/(4\pi R_A^3)$ is the density and $\delta_A = (N-Z)/A$.

Compressible liquid-drop model:

$$e_{UM}(n_A, \delta_A) = E_{sat} + \frac{1}{2}K_{sat}x^2 + \frac{1}{2}e_{sym,2}(n_A)\delta_A^2 \qquad \text{with } x = \frac{n - n_{sat}}{3n_{sat}}$$

Leptodermous expansion for K_A

$$K_A = K_{sat} + K_\tau \delta^2 + K_{Coul}\frac{Z^2}{A^{4/3}} + K_{surf}A^{-1/3} + \dots$$

Blaizot, PR 64, 171 (1980)

Derivation of K_A from the CLDM:

We have: $K_A \equiv 9n_A \frac{\partial^2(e_A n_A)}{\partial n_A^2} = R_A^2 \frac{\partial^2 e_A}{\partial R_A^2}$ since $P_A = 0$

We obtain: $K_{Coul} = \frac{3}{5}\frac{e^2}{r_0}\left(8 + \frac{Q_{sat}}{K_{sat}}\right)$

$$K_{surf} = 4\pi r_0^2 \left\{ 2\sigma_{surf}\left(11 + \frac{Q_{sat}}{K_{sat}}\right) - 3n_A \underbrace{\frac{\partial \sigma_{surf}}{\partial n_A}}_{=0} \left(10 + \frac{Q_{sat}}{K_{sat}}\right) + 9n_A^2 \underbrace{\frac{\partial^2 \sigma_{surf}}{\partial n_A^2}}_{=0} \right\}$$

since $\sigma_{surf}(\delta_A)$

CLDM/eCLDM approach

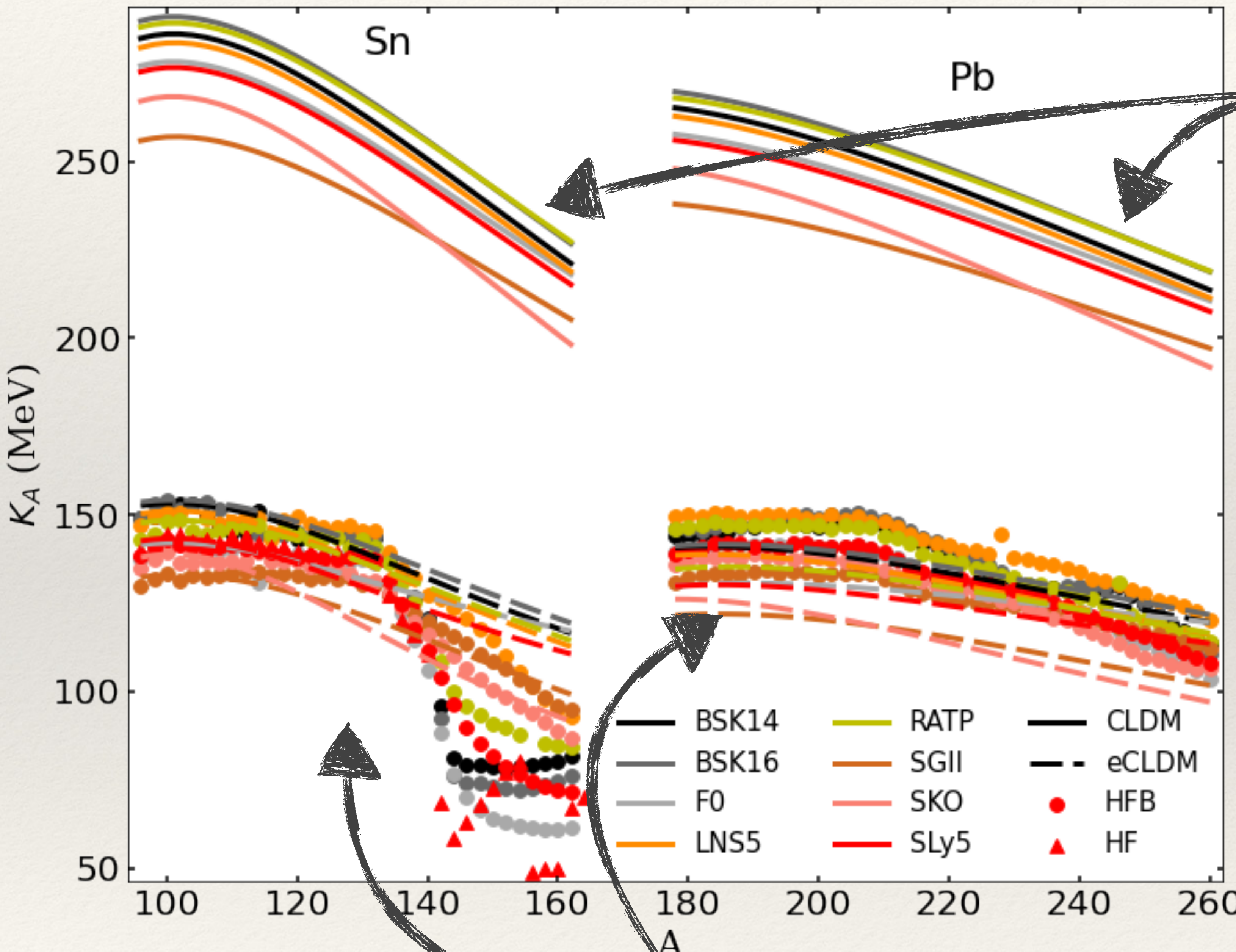

Prediction for the CLDM
+ optimisation on the nuclear chart

We then introduce a density dependence in the surface term as (eCLDM):

$$\sigma_{surf}(\delta_A)\left[1 + a_{surf} f(A) x_A^2\right]$$

with $x_A = \dfrac{n_A - n_{sat}}{3n_{sat}}$

where a_{surf} is fitted to ^{100}Sn:

	$K_{A,CHFB}(^{100}\text{Sn})$ MeV	a_{surf}
BSK14[24]	153.6	-19.95
BSK16[25]	154.4	-20.00
F0[26]	142.3	-19.90
LNS5[27]	150.7	-20.95
RATP[28]	147.9	-20.85
SGII[29]	133.2	-19.55
SKI2[30]	155.2	-20.00
SKO[31]	139.3	-19.55
SLy5[32]	142.8	-20.05

Finally we obtain

Grams, Somasundaram, JM, Khan, arXiv 2207.01884 (nucl-th)

Confrontation to data

Loss functions:

$$\chi_E^2 = \frac{1}{N_E} \sum_i \left(\frac{E_i^{exp} - E_i^{eCLDM}}{\delta E_i^{exp}} \right)^2$$

with E_i^{exp} from AME2020.

$$\chi_K^2 = \frac{1}{N_K} \sum_i \left(\frac{K_i^{exp} - K_i^{eCLDM}}{\delta K_i^{exp}} \right)^2$$

	E_{ISGMR} (MeV) from Ref. [5]	E_{ISGMR} (MeV) (this work)	R_A (fm) (SLy5)	K_A (MeV) from Eq. (1)
^{90}Zr	$17.58^{+0.06}_{-0.04}$	17.62 ± 0.07	4.256	135.6 ± 1.1
	$17.66^{+0.07}_{-0.07}$			
^{92}Zr	$17.71^{+0.09}_{-0.07}$	17.62 ± 0.12	4.293	138.0 ± 1.9
	$17.52^{+0.04}_{-0.04}$			
^{94}Zr	$15.75^{+0.27}_{-0.15}$	15.80 ± 0.21	4.330	112.9 ± 3.0
^{112}Sn	$15.23^{+0.26}_{-0.14}$	15.69 ± 0.44	4.556	123.2 ± 6.9
	$16.10^{+0.10}_{-0.10}$			
^{114}Sn	$15.90^{+0.10}_{-0.10}$	15.90 ± 0.10	4.585	128.2 ± 1.6
^{116}Sn	$15.70^{+0.10}_{-0.10}$	15.70 ± 0.10	4.614	126.5 ± 1.6
^{118}Sn	$15.60^{+0.10}_{-0.10}$	15.60 ± 0.10	4.641	126.4 ± 1.6
^{120}Sn	$15.50^{+0.10}_{-0.10}$	15.50 ± 0.10	4.667	126.2 ± 1.6
^{122}Sn	$15.20^{+0.10}_{-0.10}$	15.20 ± 0.10	4.691	122.6 ± 1.6
^{124}Sn	$14.33^{+0.17}_{-0.14}$	14.72 ± 0.40	4.715	116.2 ± 6.3
	$15.10^{+0.10}_{-0.10}$			
^{132}Sn†	14.80	14.80	4.803	121.8
^{204}Pb	$13.70^{+0.10}_{-0.10}$	13.70 ± 0.10	5.516	137.7 ± 2.0
^{206}Pb	$13.60^{+0.10}_{-0.10}$	13.60 ± 0.10	5.532	136.5 ± 2.0
^{208}Pb	$13.50^{+0.10}_{-0.10}$	13.50 ± 0.10	5.548	135.3 ± 2.0

†Fictitious data.

Grams, Somasundaram, JM, Khan, arXiv 2207.01884 (nucl-th)

Exploration of the parameter space (MCMC)

	E_{sat} (MeV)	n_{sat} (fm^{-3})	K_{sat} (MeV)	Q_{sat} (MeV)	Z_{sat} (MeV)	E_{sym} (MeV)	L_{sym} (MeV)	K_{sym} (MeV)	Q_{sym} (MeV)	Z_{sym} (MeV)
From Ref. [3]	-15.8±0.3	0.155±0.005	230±20	300±400	-500±1000	32± 2	60±15	-100±100	0± 400	-500±1000
dist1f and dist2f	-15.8	0.155	[210,250]	[-1800,600]	-500	32	[40,60]	[-300,100]	0	-500
dist3f	-15.8	0.155	[210,250]	[-1800,600]	-500	32	[80,100]	[-300,100]	0	-500

Use of flat (unbiased) prior

Exploration of different scenarios:

1- dist1 & dist1f: all known experimental data are considered for K_A ($^{90,92}Zr$, $^{112\text{-}124}Sn$ and $^{204\text{-}208}Pb$).

2- dist2 & dist2f: same as dist1 & dist1f but considering a fictitious value for K_A in ^{132}Sn.

3- dist3 & dist3f: same as dist2 \& dist2f but considering a large prior for L_{sym}.

Grams, Somasundaram, JM, Khan, arXiv 2207.01884 (nucl-th)

Results

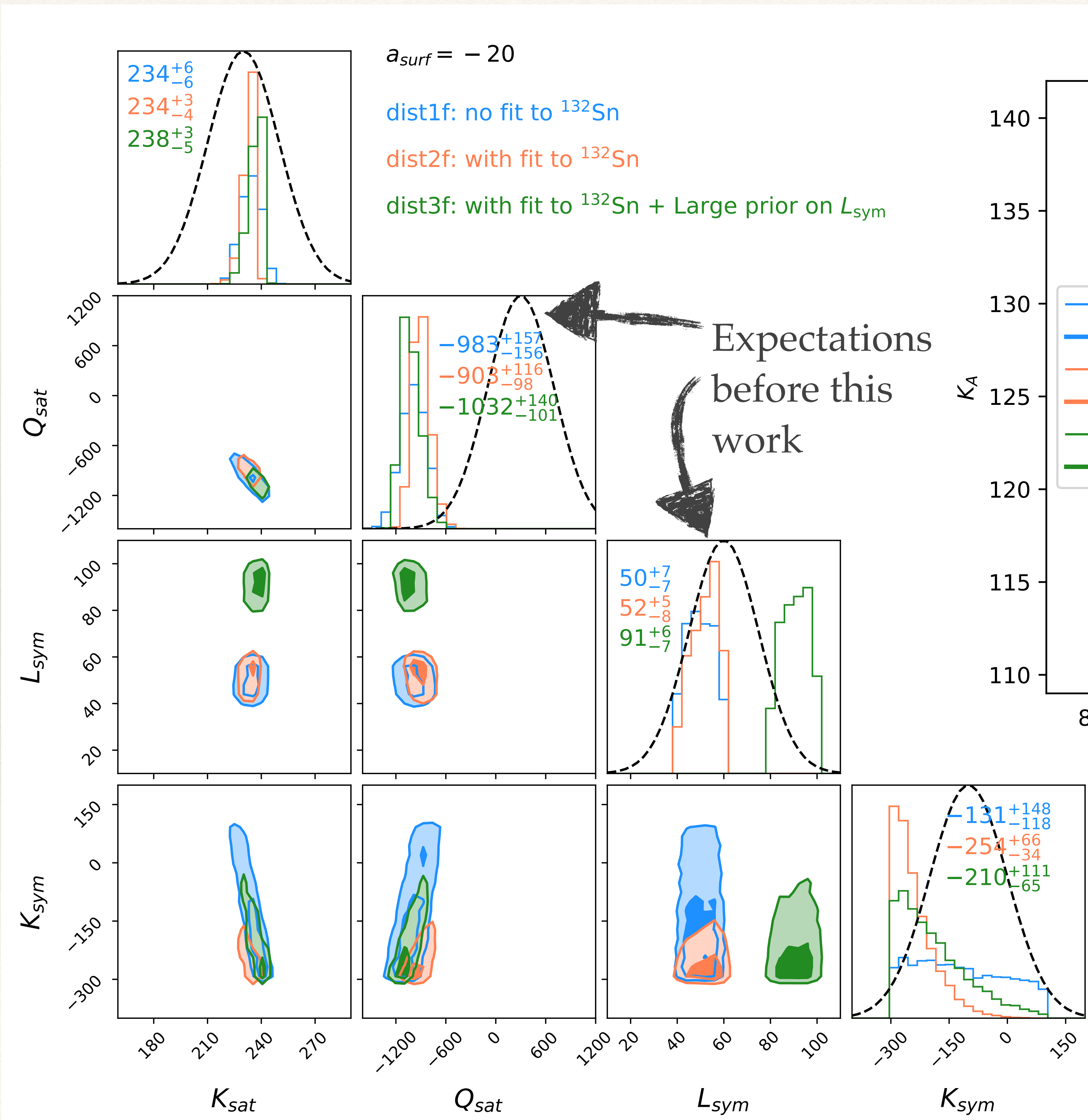

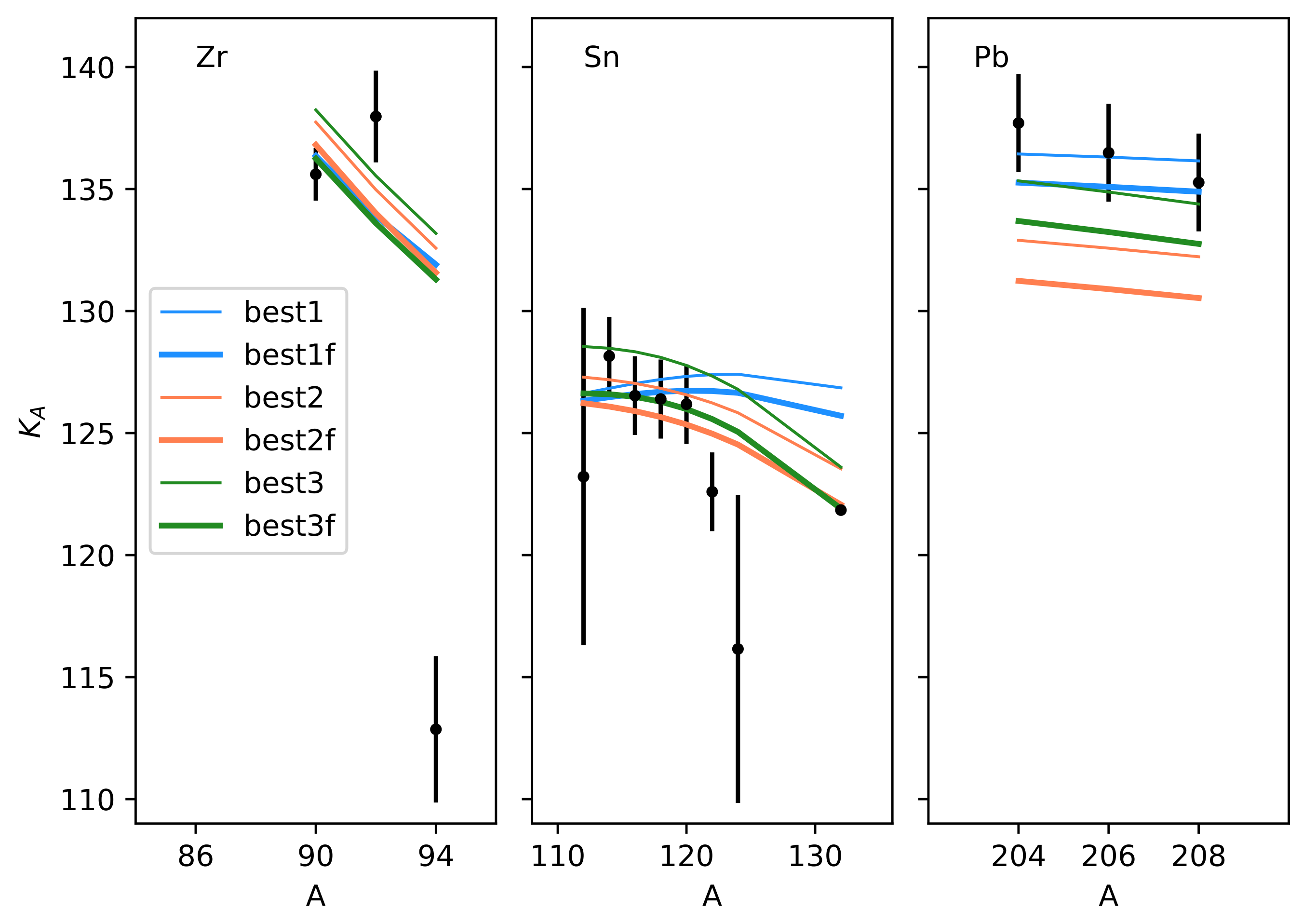

Grams, Somasundaram, JM, Khan, arXiv 2207.01884 (nucl-th)

Results

No fine-tuning to finite nuclei

With fine-tuning to finite nuclei

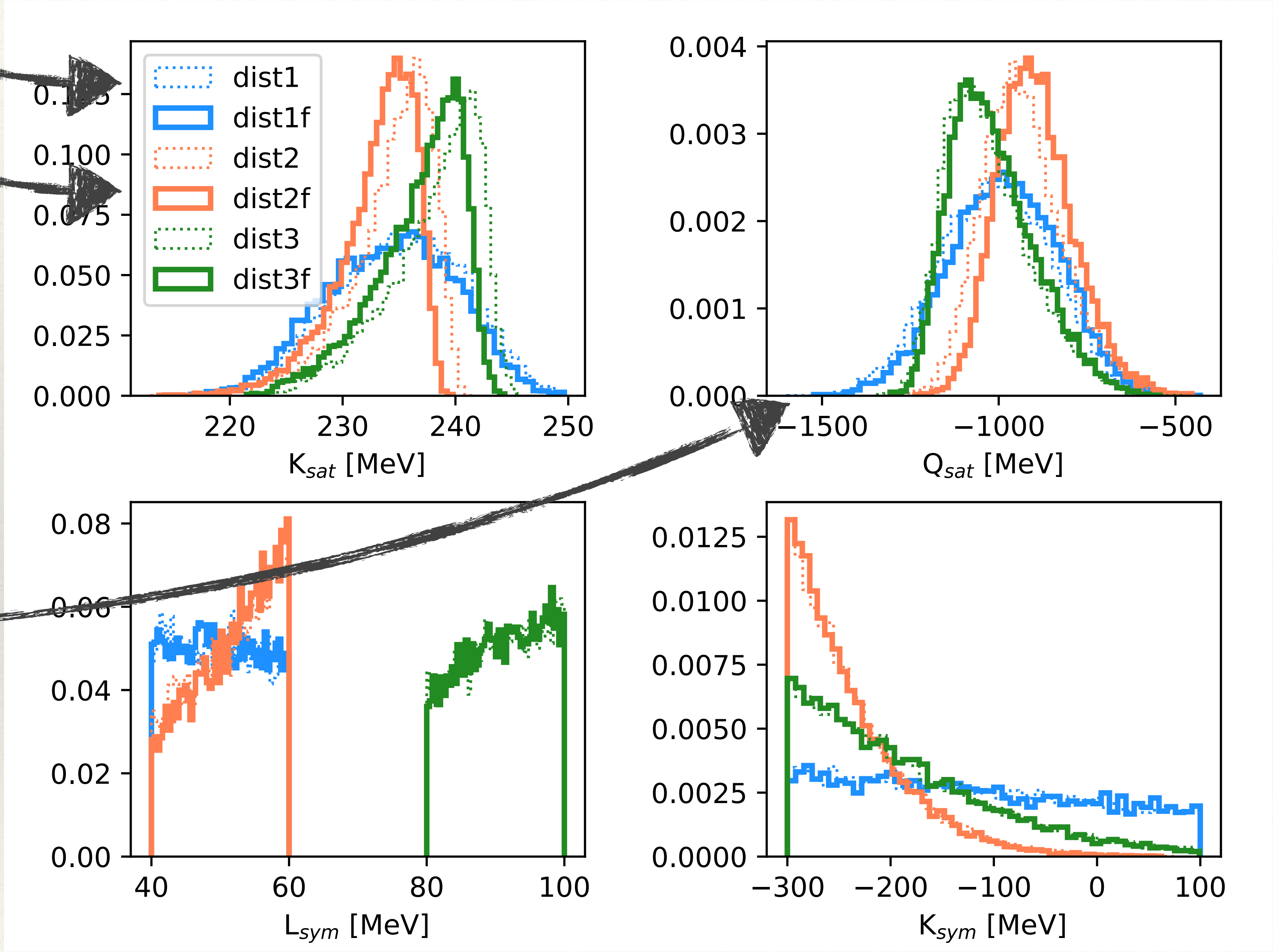

Since good low-order NEP has been chosen **and fixed**, the fine-tuning to finite nuclei is not necessary.

The Q_{sat} PDF is peaked for very low values!
Far from the usual ones given by phenomenological forces.

Possible explanation of their difficulty to accurately describe Zr, Sn and Pb data all together.

Grams, Somasundaram, JM, Khan, arXiv 2207.01884 (nucl-th)

Results

With fictitious data for ^{132}Sn

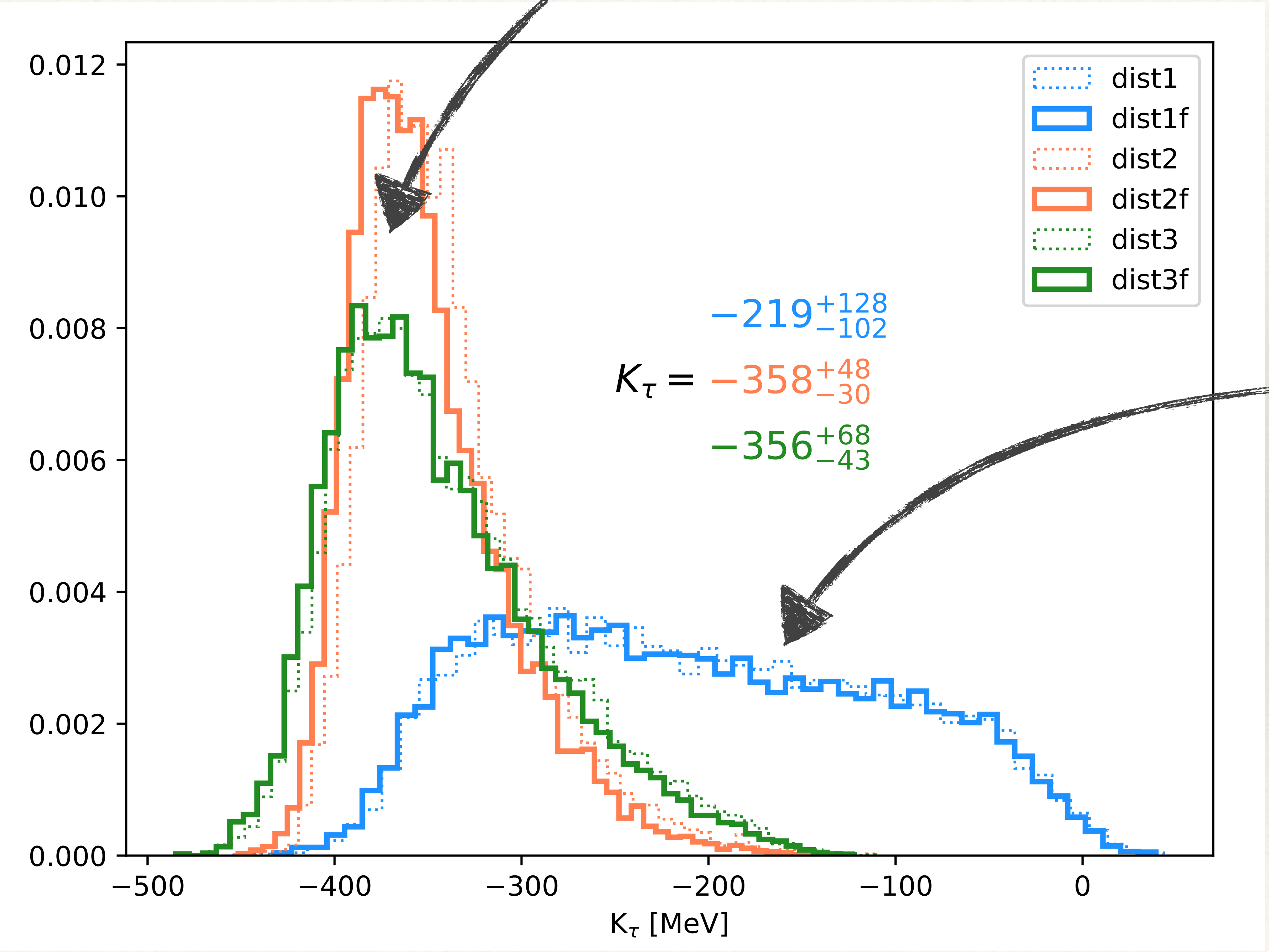

Without fictitious data for ^{132}Sn

Grams, Somasundaram, JM, Khan, arXiv 2207.01884 (nucl-th)

Sound speed in finite nuclei

$$c_{s,A} = \frac{9K_A}{h_A}$$

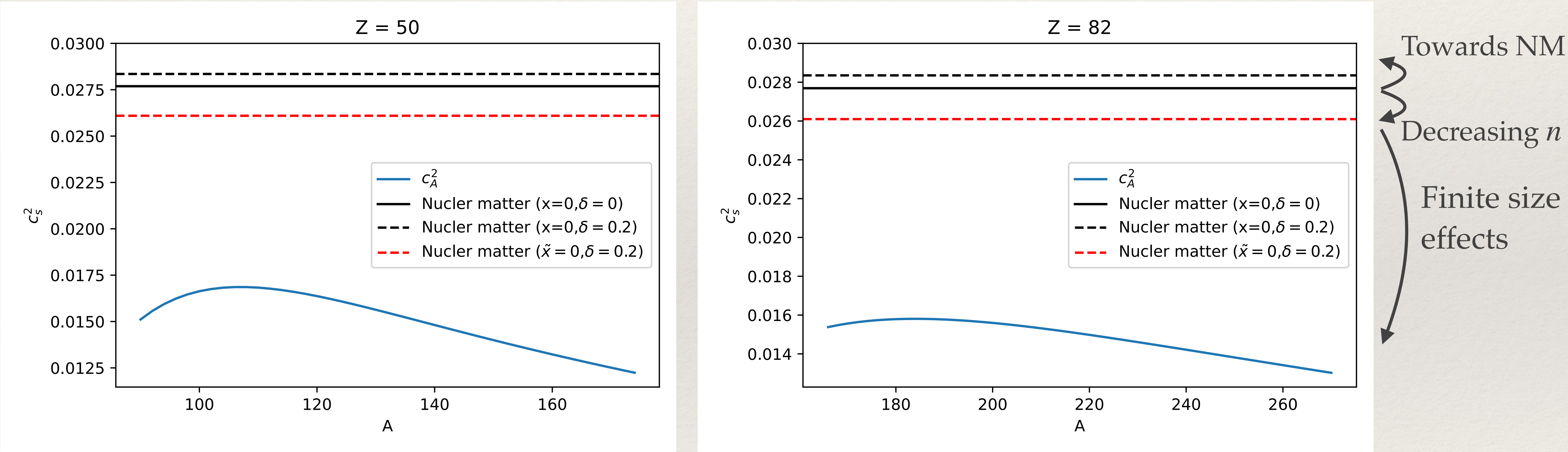

We find that $c_{s,A} \approx 0.5c_s$, mostly due to finite size terms.

Grams, Somasundaram, JM, Khan, arXiv 2207.01884 (nucl-th)

Sound speed in finite nuclei

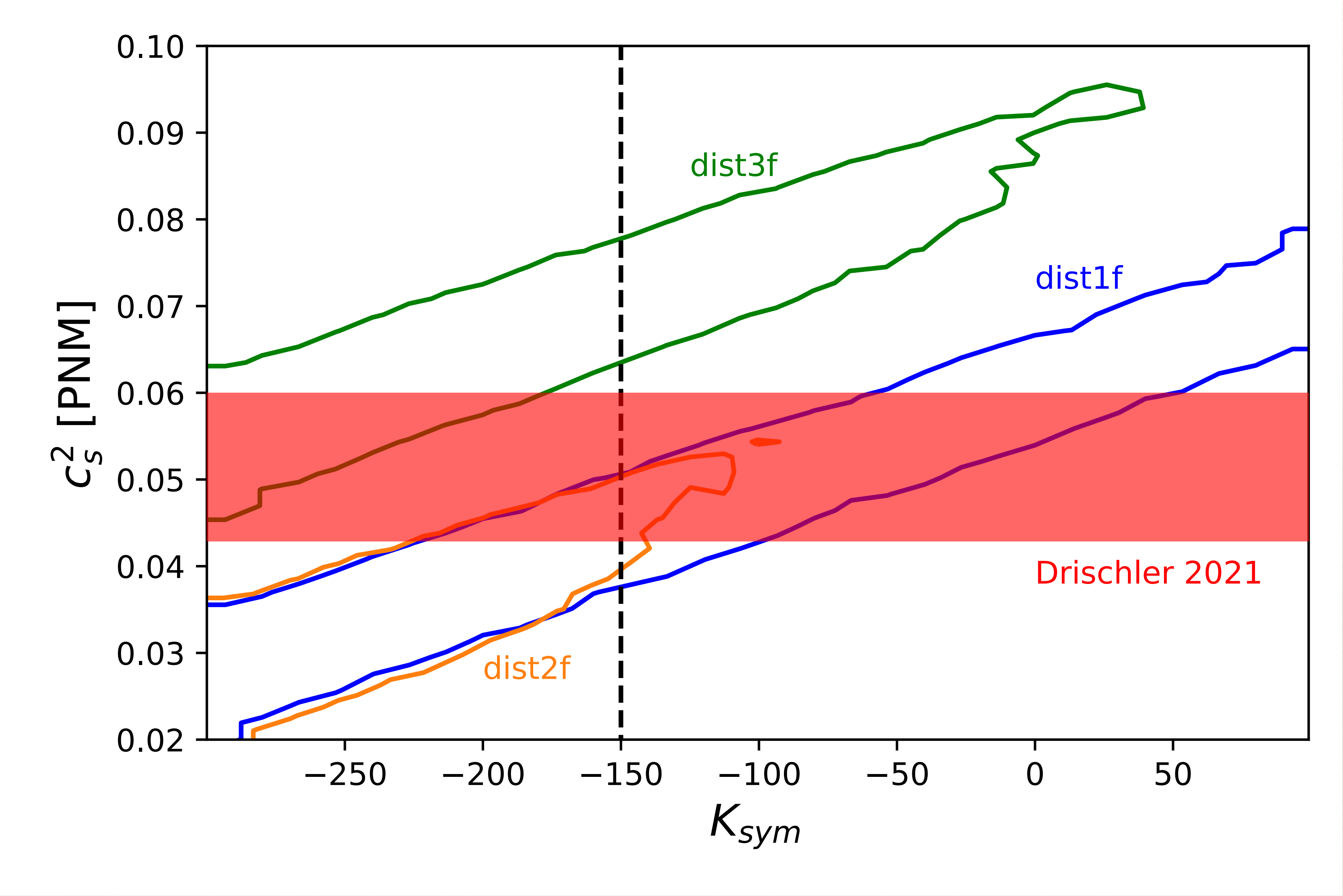

dist3f (large L_{sym}) excluded by xEFT + unitary gas limit.
A small fraction of dist2f is viable.

Grams, Somasundaram, JM, Khan, arXiv 2207.01884 (nucl-th)

Conclusions

The impact of the uncertainties in K_{sat} on the dense matter EoS is small.
However, the next NEP Q_{sat} is unknown and have a large impact on the dense matter EoS.
-> It is important to better determine Q_{sat}.

Hypothesis: Q_{sat} could be determined from E_{GMR}.

The model dependence of E_{GMR} and the difficulty to reproduce Sn and Pb with the same functional may be due to Q_{sat}.
Q_{sat} acts differently in Sn and Pb since $\langle n \rangle_A$ is different -> induces a A-dependence of E_{GMR}.

With an eCLDM approach, we were able to extract (MCMC approach) the best value for Q_{sat}.
We found that $Q_{sat} \approx -950$ MeV is optimal to reproduce Zr, Sn and Pb isotopes.

We also found a big impact of finite-size effect on the sound speed in finite nuclei:
$c_{s,A} \approx 0.5 c_s$.